Studies On The Structural, Morphological, Optical, Magnetic Characterizations and Catalytic Oxidation Of Benzyl Alcohol Into Benzaldehyde Using $Coal_2o_4$ Catalysts Prepared By Microwave Combustion And Solution Combustion Methods.

*Dr. S. Jayasree, **Suganthi.P, ***C.Veerasusaretha
*Professor, Department of Chemistry
**Assistant Professor, Department of Chemistry
*Prince Venkateshwara Padmavathy Engineering College, Ponmar
**Prince Dr.K.Vasudevan College of Engineering & Technology, Chennai.
***Faculty, Prince Shri Venkateshwara Arts and Science College, Gowriwakkam.

Abstract

Spinel $CoAl_2O_4$nano- and microstructures were successfully synthesized by a facile microwave combustion (MCM) and solution combustion (SCM) methods, respectively, using urea as the fuel. Powder XRD, FT-IR, EDX spectra, SAED, HR-SEM and HR-TEM results showed that the as-prepared samples were pure phase spinel $CoAl_2O_4$nano- and microstructures without any other secondary phase impurity. The optical band gap value of the samples $CoAl_2O_4$-MCM and $CoAl_2O_4$-SCM are 3.72 eV and 3.39 eV respectively, which were measured from UV-Visible DRS and PL spectroscopy. The magnetic properties of the samples were measured by VSM analysis. The relatively lower M_s (19.34×10^{-3} emu/g) of $CoAl_2O_4$-SCM shows that it is weak ferromagnetic in nature and high M_s (43.26×10^{-3} emu/g) of $CoAl_2O_4$-MCM confirms its ferromagnetic behavior. The sample $CoAl_2O_4$-MCM prepared by the MCM route was found to possess a higher surface area, and lower crystallite size than the $CoAl_2O_4$-SCM prepared by the SCM route, which in turn leads to the improved performance towards the selective oxidation of benzyl alcohol into benzaldehyde, with high activity, good reusability, remarkable stability and environmentally friendly and also promising materials for the industrial applications. It was found that the sample $CoAl_2O_4$-MCM show higher conversion (95.73 %) of benzyl alcohol into benzaldehyde than the sample $CoAl_2O_4$-SCM (64.52 %). Microwave irradiation has produced sufficient energy for the

formation of spinel $CoAl_2O_4$nanostructures than SCM route, because of its homogeneous distribution of microwaves within the raw materials.

Key words : MCM,SCM,NANO STRUCTURES,POROUS,SPINEL.

4.2.1. Introduction

Nowadays, binary transition metal oxides or complex oxides with spinel structure AB_2O_4, where A and B stand for two different cations such as divalent (Zn^{2+}, Cu^{2+}, Mn^{2+}, Ni^{2+}, etc.) and trivalent (Al^{3+}, Fe^{3+}, etc.) cations, respectively, are a class of chemically and thermally stable materials, which are suitable for a wide range of applications such as optical, ceramics, magnetic and catalysis [1, 2]. Among them, spinel cobalt aluminate ($CoAl_2O_4$) is most attractive inorganic blue pigments, because of their unique properties such as high thermal, chemical, solar and atmospheric stabilities, high mechanical resistance, hydrophobicity, and low surface acidity with impressive optical, dielectric, and sensing properties [1-8]. $CoAl_2O_4$ has a cubic spinel structure with a space group of *Fd3m* (lattice constant a = 8.1 Å), Co^{2+} ions occupy the tetrahedral (A) sites, whereas Al^{3+} ions are accommodated in octahedral (B) sites [9].

Recently, several synthetic methods to synthesize spinel $CoAl_2O_4$nano- and microstructures, generally requires long time and high-temperature (~1000 °C), such as sol-gel, sono chemical, co-precipitation, hydrolysis, hydrothermal, solvothermal, combustion and polymerized complex methods [9-15]. Feldmann [5] reported blue $CoAl_2O_4$ by two step process by polyol method to obtain purple colored product by refluxing at 180 °C in diethylene glycol and followed by heat-treatment at 600 °C to obtain blue colored $CoAl_2O_4$. Rangappa*et al.* [6, 7] reported the synthesis of spinel $CoAl_2O_4$nanocrystals under supercritical condition in aqueous medium at ~ 400 °C and high pressure. However, the above conventional techniques meet some disadvantages such as long synthesis time and high-energy consuming, requirement of complicated equipment and complex procedures, difficult in their operation and present low yield and also required high temperature for calcinations to complete the crystallization

of the final products with spinel structure [16]. Also, lead to the presence of some toxic chemical (surfactants, templates and catalysts) species adsorbed on the surface that may have poor result in medical applications. Among the above conventional strategies, easy and cost effective methods to synthesize the spinel aluminates by employment of economical, non-toxic and environmentally gentle precursors are still the key issue. Hence, the growth of simplistic and eco-friendly caring preparation route is severely crucial and favored with low energy cost [17].

A special attention has been committed to the synthetic procedures of spinel aluminates with reduced cost production connected with an enhanced feature of materials by combustion methods. Nowadays, combustion synthesis is considered one of the most reachable, rapid, and economic soft method for the synthesis of simple and mixed metal oxides which afford highly crystalline and pure materials with unique properties. The thermally encouraged redox reaction between an oxidant (metal nitrates) and a fuel (organic molecule which ignites the reaction) is self-sustained, uses relatively simple equipments and generally low cost reactants. The thermo chemical characteristics of the fuels represent significant issues of the combustion methods, influencing the flame temperature through the entire combustion process [18-22].

Recently, the microwave combustion method (MCM), the use of microwave energy as a heating source for the combustion methods has been engaged, due to its fast reaction kinetics, cleanliness, efficiency and effectiveness. In this method, preparation of such active nanostructures is easy, fast and low energy with soft method than the above said conventional methods. Also, due to the homogeneous distribution of microwave heating, this results the different morphologies of the final products with higher surface area and smaller crystallite size of the final products [23, 24]. However, this method is simple and fascinating route toward all classes of oxide materials, due to the yields of the final products of metal oxides are associated with their special structural personalities, namely nanosized dimensions and unique microstructures. Besides, to our knowledge, no literature is available on the synthesis, structural,

morphological, optical, magnetic and catalytic properties of spinel $CoAl_2O_4$ nanostructures by a simple microwave combustion method using glycine as the fuel.

Spinel $CoAl_2O_4$nano- and microstructures have been widely used in catalysis as a heterogeneous catalyst and reused several times and it can be recovered easily from the reaction mixture by simple filtration method. Moreover, $CoAl_2O_4$ is non-toxic, inexpensive, relatively high surface area make them fitting for use as cost-effectively and eco-friendly viable solid heterogeneous catalyst. Spinel $CoAl_2O_4$ have applied as a catalyst in the oxidations of CO and decomposition of H_2O_2 over heterogeneous catalysts and its low cost, environment friendly and nontoxic character as well as catalyst is highly admirable [25-32]. The as-prepared spinel $CoAl_2O_4$nano- and microstructures were investigated for structural, morphological, optical, magnetic and catalytic properties and different characterizations have been carried out using X-ray diffraction (XRD), Fourier transform infrared (FT-IR) analysis, high resolution scanning electron microscopy (HR-SEM), high resolution transmission electron microscopy (HR-TEM), energy dispersive X-ray spectroscopy (EDX), Brunauer-Emmett-Teller (BET) analysis, UV-Visible diffuse reflectance spectra (DRS), photoluminescence (PL) spectra and vibrating sample magnetometer (VSM) techniques and the obtained results are presented here.

4.2.2. Experimental part

4.2.2.1 Preparation of $CoAl_2O_4$nano- and microstructures by microwave combustion (MCM) and solution combustion (SCM) methods

All the chemicals used in this study were of analytical grade obtained from Merck, India and were used as received without further purification. All chemicals such as nitrates of cobalt and aluminum, and urea were used as the fuel for this method. The stoichiometry of metal nitrate salts and fuel was calculated based on the total oxidizing and reducing valencies related to the oxidant agents and to the fuels. Initially, the precursor mixture of nitrates solution in glycine was placed in a domestic microwave oven and exposed to the microwave energy in a 2.45 GHz multimode cavity at 850 W for 10 minutes.

When the solution attained the point of spontaneous combustion, ignition took place resulting in a rapid flame and yielding solid fluffy final products. The obtained solid powders were washed well with water and ethanol several times and dried at 80 ºC for 1 h, and labeled as $CoAl_2O_4$-MCM, and then used for further characterizations. In the next separate experiment, solution combustion method (SCM), the same reaction mixture was taken in the silica crucible and treated in an air furnace at 500 °C for 2 h at a heating rate of 5°C/min, and cooled at the same rate; it became solid, which was labeled as $CoAl_2O_4$-SCM.

4.2.2.2 Characterizations of spinel $CoAl_2O_4$nano- and microstructures

The structural characterization of spinel $CoAl_2O_4$nano- and microstructures was performed using a Philips X'pert X-ray diffractometer with CuKα radiation at

λ = 1.540 Å. Structural refinements using the Rietveld method were carried out using PDXL program, and both refined lattice parameter and crystallite size of the obtained spinel $CoAl_2O_4$ samples were reported. The surface functional groups were analyzed by Perkin Elmer FT-IR spectrometer. Morphological studies and energy dispersive X-ray (EDX) analysis of spinel $CoAl_2O_4$samples have been performed with a Jeol JSM6360 high resolution scanning electron microscope. The transmission electron micrographs were carried out by Philips-TEM (CM20). The surface area was derived from the N_2 adsorption-desorption isotherms using liquid nitrogen at 77 K using an automatic adsorption instrument (Quanta chrome Corp. Nova-1000 gas sorption analyzer). The UV-Visible diffuse reflectance spectrum of spinel $CoAl_2O_4$samples was recorded using Cary100 UV-Visible spectrophotometer to estimate their band gap energy (E_g). The photoluminescence (PL) properties were recorded at room temperature using Varian Cary Eclipse Fluorescence Spectrophotometer. The magnetic properties were investigated at room temperature in an applied magnetic field sweeping from -10 to +10 KOe using a PMC Micro Mag 3900 model vibrating sample magnetometer (VSM) equipped with 1 Tesla magnet.

4.2.3. Results and discussion

4.2.3.1 Structural analysis

The powder X-ray diffraction (XRD) analysis was used to characterize the phase purity and crystal structure of the as-prepared spinel $CoAl_2O_4$ samples. Fig. 4.2.1a,b shows the XRD pattern of the samples $CoAl_2O_4$-MCM and $CoAl_2O_4$-SCM, respectively. The peaks at 2θ values of 31.23°, 36.86°, 38.68°, 44.96°, 49.02°, 55.73°, 59.41°, 65.34°, 74.28°, and 77.44° correspond to the (220), (311), (222), (400), (331), (422), (511), (440), (620) and (533) planes, respectively, and could be readily assigned to a cubic phase spinel $CoAl_2O_4$ structure (space group *Fd3m*, with lattice size of 8.106 Å) [9].According to the XRD patterns, all diffraction peaks can be perfectly indexed as centered cubic spinel $CoAl_2O_4$is in agreement with JCPDS card no. 44-0160 [33, 34]. Furthermore, no other crystalline diffraction peaks were present in the XRD pattern, indicating the formation of highly pure $CoAl_2O_4$. Therefore, the XRD patterns confirm the diffraction lines of single phase of $CoAl_2O_4$ with a characteristic cubic spinel structure, and no secondary phases (CoO and Al_2O_3) were detected. Furthermore, the examination revealed that both samples $CoAl_2O_4$-MCM and $CoAl_2O_4$-SCM show sharp peaks, which indicating good crystallinity.

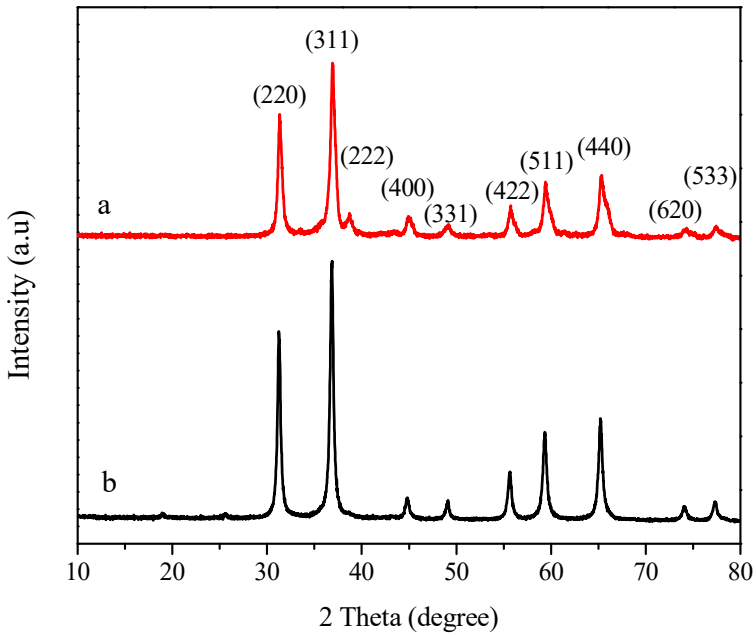

Figure 4.2.1. XRD pattern of $CoAl_2O_4$: (a) $CoAl_2O_4$-MCM (b) $CoAl_2O_4$-SCM

The average crystallite size of spinel $CoAl_2O_4$nano- and microstructures were calculated using Debye Scherrer formula,

$$L = \frac{0.89\lambda}{\beta \cos\theta} \quad \text{---- (1)}$$

where L is the crystallite size, λ , the X-ray wavelength, θ, the Bragg diffraction angle and β, the full width at half maximum (FWHM). The average crystallite size of the sample $CoAl_2O_4$-MCM (13.46 nm) is lower than that of the sample $CoAl_2O_4$-SCM (34.79 nm), which are calculated from the full-width at half-maximum of the (311) plane (Table 4.2.1). The observed higher crystallite size of $CoAl_2O_4$-SCM is mainly due to the high temperature calcinations (500 °C for 2 h), than the sample $CoAl_2O_4$-MCM. Nevertheless, the MCM approach produces spinel $CoAl_2O_4$ in a microwave-oven operated at a power of 850 W generated the temperature ranging from 150 to 400 °C that would results the formation of spinel $CoAl_2O_4$ nanostructures within 10 minutes with smaller crystallite size. However, the diffraction peaks for the sample $CoAl_2O_4$-MCM is slightly broadened than the sample $CoAl_2O_4$-SCM, due to the smaller crystallite size, with the increase in heat-treatment temperature (SCM route), the diffraction lines become narrower and more intense resulted higher crystallite size ($CoAl_2O_4$-SCM). Also, the broad reflection peaks proved very fine crystallite size of the spinel $CoAl_2O_4$synthesized by the MCM route. But, in the SCM approach, the raw materials are kept at 500 °C for 2 h, thus allowing the formation of pure $CoAl_2O_4$ microstructures. This can be further understood by heat-treating at higher temperature (500 °C) to enhance the crystallite size of $CoAl_2O_4$ spinel. As expected, the 500 °C heat-treated sample showed further enhancement of $2\theta = 37.03°$ peak intensity (Figure 4.2.1b) suggesting higher crystallite size of $CoAl_2O_4$. The crystallite size however lower in case of $CoAl_2O_4$-MCM sample compared to the $CoAl_2O_4$-SCM treated powder [9].

Table 4.2.1. Lattice parameter, crystallite size and band gap values of spinel $CoAl_2O_4$ nano and microcrystals.

Samples	Crystallite size (nm)	Lattice parameter (Å)
$CoAl_2O_4$-MCM	13.46	8.106
$CoAl_2O_4$-SCM	34.79	8.101

4.2.3.2. Fourier transform infrared (FT-IR) analysis

Fig. 4.2.2a, b shows the FT-IR spectra of the samples $CoAl_2O_4$-MCM and $CoAl_2O_4$-SCM, respectively. The spectral vibration bands corresponding to the spinel structure was appeared at 653 and 561 cm^{-1}. Both the samples, the metal-oxygen stretching frequencies appeared in the range of 500-700 cm^{-1}, associated with the vibrations of Co-O, Al-O and Co-O-Al bonds [35, 36]. The observed results are in good agreement with the powder XRD analysis. A strong and broad absorption band centered in the region 3000-3500 cm^{-1}, which can be assigned to the vibrations of water molecules absorbed from atmosphere.

The absorption band at 2343 cm^{-1} is due to the stretching vibration of CO_2 from atmosphere. A band at around 1630 cm^{-1} is present in both samples, which can be assigned to the H-O-H bending vibration. A small band appeared at 1487 cm^{-1} is associated with the –C-H stretching vibrations. The observed results suggested that the formation of spinel $CoAl_2O_4$

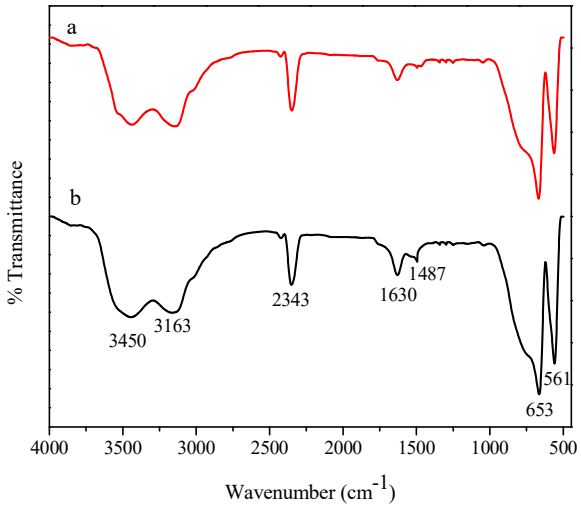

Figure 4.2.2.FT-IR spectra of $CoAl_2O_4$: (a) $CoAl_2O_4$-MCM (b) $CoAl_2O_4$-SCM

4.2.3.3 Scanning electron microscopy (SEM) studies

The surface morphology of the samples was investigated by the high resolution scanning electron microscope (HR-SEM) technique. Fig. 4.2.3a, b shows the HR-SEM images of the sample $CoAl_2O_4$-MCM, which confirmed the presence of particle-like nano-structured morphology with agglomeration. It reveals that the nanoparticles are homogeneous and grains are distributed uniformly with smaller particles and large agglomerates with diameter ranging below 25 nm, due to the fact that the MCM reaction is volumetric and uniform heating method, when compared to the SCM route, which is non-uniform and radiative method. Fig. 4.2.3c, d shows the HR-SEM images of the sample $CoAl_2O_4$-SCM, which confirmed the presence of agglomerated micro-crystals. Therefore, we can infer that the agglomerated $CoAl_2O_4$nano- and microcrystals formed during the MCM and SCM approaches, respectively. Thus, the higher temperature and non-uniform heating method of SCM reaction in a furnace caused grain growth with micro-crystals than MCM route. However, the MCM route is volumetric and uniform heating method, which prevents grain growth, thus gives nano-structured morphology. Moreover, the sample $CoAl_2O_4$-SCM is exposed for more time, and it results in the formation of agglomeratedmicro-crystals (may be due to the sintering effect). The average particles size of the sample $CoAl_2O_4$-MCM is smaller

than 25 nmand it is slightly larger than crystallites size determined by powder XRD, which shows that every particle is formed by a number of crystallites or grains. There is a direct connection between the XRD crystallite size and particle size of SEM image, meaning that a particle can be formed by agglomeration of crystallites. However, decomposition of raw materials by different methods has considerable effects on the morphology of the final products. Also, illustrates how the particle size can be successfully controlled by setting the growth temperature. Instantaneously, microwaves may also play a key role in controlling the morphology of the samples.

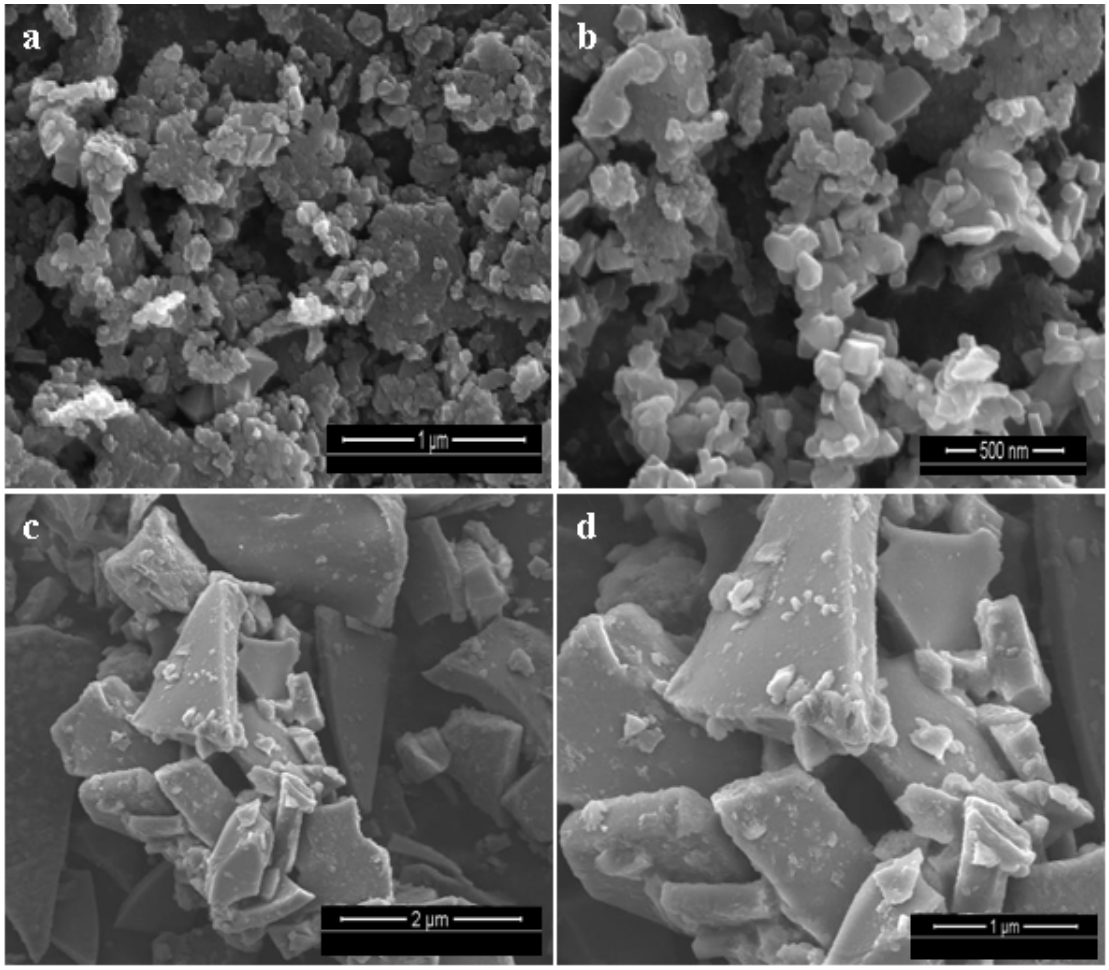

Figure 4.2.3. HR-SEM of $CoAl_2O_4$: (a, b) $CoAl_2O_4$-MCM and (c, d) $CoAl_2O_4$-SCM

4.2.3.4 Transmission electron microscopy (TEM) studies

To provide further evidence for the formation of nanoparticles-like morphology of $CoAl_2O_4$-MCM, high resolution transmission electron microscopy (HR-TEM) analysis was carried out only for $CoAl_2O_4$-MCM sample and is shown in Fig. 4.2.4a, b. The average size and void space diameter of single $CoAl_2O_4$ nanoparticles is found to be in the range of 10-15 nm. The obtained nanoparticles are nearly spherical shaped with a uniform size distribution. It may be due to the fact that spinel $CoAl_2O_4$ was prepared within a short reaction time of 10 min by means of a domestic microwave oven operated at 2.45 GHz (850W). It is concluded that the temperature is a key factor in the controlled synthesis of nano-sized materials. Herein, $CoAl_2O_4$ nanoparticles were prepared by only the temperature optimization and there is no use of any other solvent or surfactant. Also, the mean particle size determined by HR-TEM is very close to the average particle size calculated by the Scherrer formula from the powder XRD pattern.

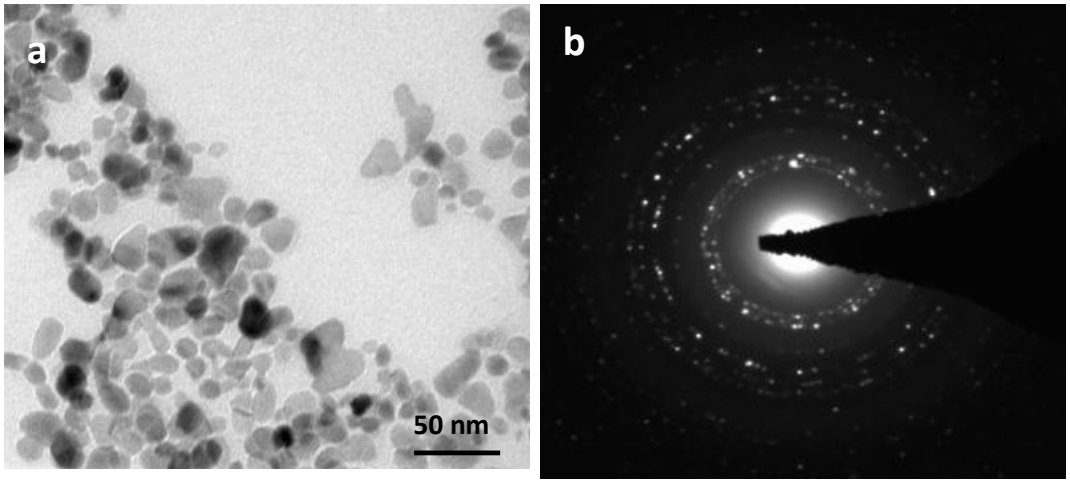

Figure 4.2.4. HR-TEM image (a) and SAED pattern (b) of $CoAl_2O_4$-MCM

A selected area electron diffraction pattern (SAED) of the spinel $CoAl_2O_4$nanoparticles is shown in the Fig. 4.2.4b. The SAED pattern implies that the prepared $CoAl_2O_4$nanoparticles are good crystalline materials with higher crystalline in nature.In order to have a idea of the adsorbance capability of spinel $CoAl_2O_4$nano- and microstructures, BET surface area was determined using N_2 adsorption/desorption studies.The surface area of the sample $CoAl_2O_4$-MCM was found to be higher i.e. 68.27 m^2/g than the

sample $CoAl_2O_4$-SCM (37.53 m^2/g), and the observed difference may be due to the smaller particle size of $CoAl_2O_4$-MCM than $CoAl_2O_4$-SCM, which is confirmed by HR-SEM and HR-TEM analysis. Therefore, it is believed that the high surface area of $CoAl_2O_4$-MCM could enhance the catalytic activity than that of the sample $CoAl_2O_4$-SCM.

4.2.3.5 Energy dispersive X-ray (EDX) analysis

The elemental composition and purity of the samples were confirmed by energy dispersive X-ray (EDX) analysis. Fig. 4.2.5a, b shows the EDX spectra of $CoAl_2O_4$-MCM and $CoAl_2O_4$-SCM samples, respectively, shows the peaks of Al, Co and O elements and there is no other peak, which is confirmed the as-prepared samples are pure and there is no other impurity. In the EDX pattern, the presence of Al, Co and O elements in proper proportions suggested that the expected stoichiometry was maintained in the prepared samples. The EDX results suggested that the precursors have fully undergone the chemical reaction to form the expected single phase product. However, a small Au (gold) peak was appeared at 2.1 KeV for both the samples and Au has been used as a sputter coating for the better visibility of the surface morphology, while preparing the sample for HR-SEM analysis.

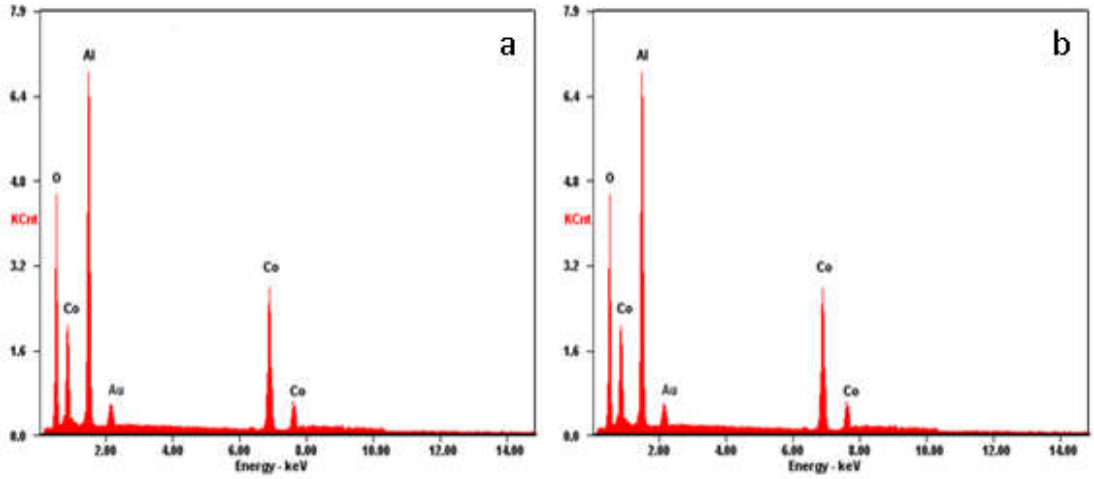

Figure 4.2.5. EDX spectrum of $CoAl_2O_4$: (a) $CoAl_2O_4$-MCM (b) $CoAl_2O_4$-SCM

The composition of the $CoAl_2O_4$ NSPs and NPLswas investigated using an energy dispersive analysis by X-rays (EDX) set up attached with scanning electron microscope.The EDAX results revealed that the following composition in at percentage.

$CoAl_2O_4$ MCM

Element	Wt%	At%
OK	09.54	27.23
AlK	57.52	48.25
CoK	32.94	24.52
Total	100 %	

$CoAl_2O_4$ SCM

Element	Wt%	At%
OK	16.79	41.41
CoK	21.23	14.35
AlK	61.98	44.23
Total	100 %	

The purity and elemental compositions of the samples was confirmed by means of energy dispersive X-ray (EDX) analysis. Fig. 4.1.3a,b show the EDX spectra of $CoAl_2O_4$-MCM and $CoAl_2O_4$-SCM respectively. It exhibited Co, Al, and O peaks and indicated the presence of $CoAl_2O_4$ phase without any other impurity. In the EDX pattern, the presence of Al, Co and O elements in proper proportions suggested that the expected stoichiometry was maintained in the prepared samples. It is in good agreement with the powder XRD analysis. The peak at 2.1 KeV in the EDX spectra were due to the gold coated on the samples before recording HR-SEM for better visibility of the surface morphology.

4.1.3.4 Powder X-ray diffraction (XRD) analysis

The powder XRD pattern of the prepared samples is given in Fig. 4.1.4. Fig. 4.1.4a,b shows the powder XRD pattern of the samples $CoAl_2O_4$-NSPs (prepared by MCM), and $CoAl_2O_4$-NPLs (prepared by SCM), respectively using urea as the fuel. It revealed that both the samples $CoAl_2O_4$-NSPs and $CoAl_2O_4$-NPLs had higher crystalline in nature. The diffraction peaks of the samples matched well with the JCPDS card no. 10-0339 [31].

M.Wt	-	176.66
Vol	-	521.27
Dx	-	4.502
System	-	Cubic $CoAl_2O_4$ (space group Fd3m)

4.2.3.6 UV-Visible diffuse reflectance spectroscopy (DRS) analysis

The fundamental process of UV-Visible absorption/reflectance/transmittance of light by metal oxide semiconductors is significant to their electronic structures. UV-Visible diffuse reflectance spectroscopy (DRS) studies play a vital role in estimating the band gap energy (E_g) of the metal oxide semiconductors. The optical energy band gap was calculated using Tauc relation [37]. The Kubelka-Munk function is generally applied to convert the diffuse reflectance into equivalent absorption coefficient and mostly used for analyzing the powder samples [38]. The Kubelka-Munk function *F(R)* was used to calculate the E_g of the nanocrystalline spinel $CoAl_2O_4$ samples. Thus, the vertical axis is converted into quantity *F(R)* which is equal to the absorption co-efficient. Thus the *'α'* in the Tauc equation is substituted with *F(R*) and hence the relation becomes,

$$\left(F(R)\right) = \alpha = \frac{(1-R)^2}{2R} \qquad \text{---- (2)}$$

where, F(*R*) is Kubelka-Munk function, *'α'* the absorption coefficient, *'R'* the reflectance. Thus, the Tauc relation becomes,

$$F(R)h\upsilon = A(h\upsilon - E_g)^n \text{---- (3)}$$

where n = 1/2 and 2 for direct and indirect transitions, respectively, thus giving direct and indirect band gaps. The plots of $(F(R)h\upsilon)^2$ versus hυ for both samples are shown in Fig. 4.2.6. Extrapolation of linear regions of these plots to $(F(R)h\upsilon)^2 = 0$ gives the direct band gap values. The direct band gap value of the sample $CoAl_2O_4$-MCM was observed to be 3.72 eV, and it is decreased with increasing the higher crystallite size of the sample $CoAl_2O_4$-SCM (E_g = 3.39 eV). The observed higher E_g value of the sample $CoAl_2O_4$-MCM is due to smaller particle size. Interestingly, the band gap energy decreased with increasing the crystallite size of the samples.

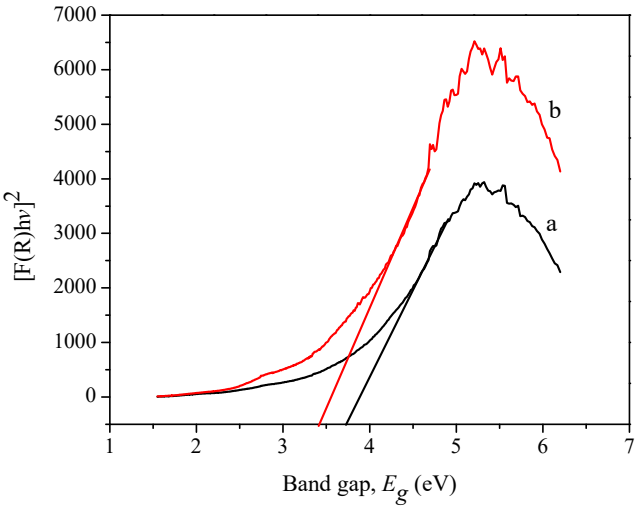

Figure 4.2.6. UV-Visible diffuse reflectance spectra (DRS) of $CoAl_2O_4$: (a) $CoAl_2O_4$-MCM (b) $CoAl_2O_4$-SCM

4.2.3.7 Photoluminescence (PL) spectroscopy

Room temperature photoluminescence (PL) spectroscopy is an important tool for investigating the electronic and optical properties of semiconducting materials. Moreover, PL spectrum gives the information about the band gap with the relative active position of sub band gap and defect states of the semiconductors [39, 40]. Fig. 4.2.7a,bdemonstrates the room temperature PL spectra recorded at λ_{ex} = 290 nm of $CoAl_2O_4$ samples prepared with two different methods namely microwave combustion and solution combustion methods, respectively. A small band is observed at 362 nm is ascribed to the near band-edge (NBE) emission of wide band gap of $CoAl_2O_4$ due to the recombination of free excitons through an exciton-exciton process. The estimated band gap (3.39 eV) from the NBE emission is in agreement with the band gap estimated from Kubelka-Munk plot derived from the UV-Visible DRS spectra. However, both the samples show a peak corresponding to violet emissions centered at 418 nm and 443 nm, due to the radiating defects related to the interface traps existing at the grain boundaries. Also, blue emissions appeared at 461 nm and 485 nm, which represent a deep level visible emissions associated with localized levels in the band gap [41, 42]. A green emission centered at 543 nm, may be ascribed to the oxygen vacancies. It is found from the PL spectra that the emission characteristics are governed by the defect controlled processes.

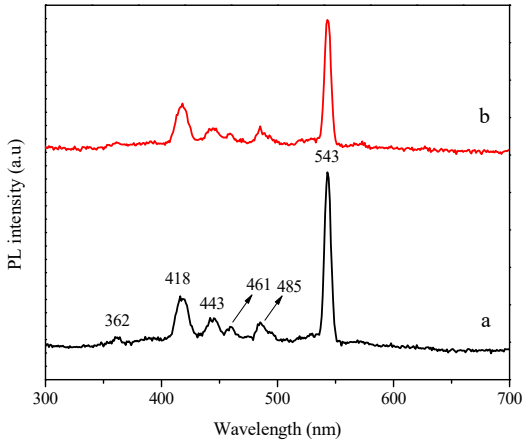

Figure 4.2.7. Room temperature PL spectra of $CoAl_2O_4$: (a) $CoAl_2O_4$-MCM (b) $CoAl_2O_4$-SCM.

4.2.3.8 VSM measurements

Fig. 4.2.8 shows the *M-H* hysteresis of the spinel $CoAl_2O_4$nano- and microstructures prepared by MCM and SCM approaches. The shape and area of the *M-H* hysteresis loops were found to depend strongly on the preparation methods as well as on the ratio of the crystalline phases in the powders. The shape of the *M-H* hysteresis loop shows a characteristic weak ferromagnetic behavior for both samples. Both the samples displayed the normal (s shaped) narrow hysteresis loops, and the magnetic parameters like saturation magnetization (M_s), remanent magnetization (M_r) and coercivity (H_c) of the samples were summarized in Table 2. From the VSM measurements, the H_c and the M_r of the sample $CoAl_2O_4$-MCM is estimated to be 299.95 O_e and 49.23 × 10^{-3} emu/g, respectively, and for the sample $CoAl_2O_4$-SCM is 278.21 O_e and 11.69 × 10^{-3} emu/g, respectively. The M_s of sample $CoAl_2O_4$-MCM (43.26 × 10^{-3} emu/g) is higher than that of sample $CoAl_2O_4$-SCM (19.34 × 10^{-3} emu/g), and both the samples are weak ferromagnetic in nature. The low H_c and M_r values confirm that the spinel $CoAl_2O_4$nano- and microcrystals have soft and weak ferromagnetic nature.

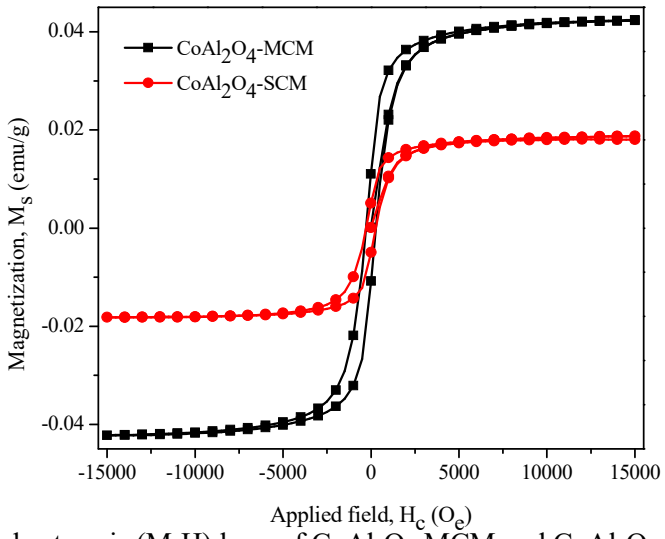

Figure 4.2.8. Magnetic hysteresis (M-H) loop of $CoAl_2O_4$-MCM and $CoAl_2O_4$-SCM samples

Spinel $CoAl_2O_4$nano- and microcrystals has a normal spinel structure with the ferromagnetic nature, due to the exchange between the ions occupying the tetrahedral (A-) and octahedral (B-) sites.

Also, it has zero net magnetization, because of the complete compensation of the sublattice magnetization [43, 44]. At room temperature, the H_c values of the sample $CoAl_2O_4$-MCM is 299.95 O_e, which is higher than the sample $CoAl_2O_4$-SCM (278.21 Oe), and it probably attribute to the high shape anisotropy of spinel $CoAl_2O_4$nano-crystals, which allow them in magnetizing in all directions along their easy magnetic axes. As a result, the different $M_s$value of spinel $CoAl_2O_4$ samples prepared by MCM and SCM methods could be related to the change in the sizes of the nano- and microcrystals. It is well known that the magnetic property of nanomaterials is strongly dependent on the shape and sizes of the particles and their crystallinity. However, it is observed that the lower H_c and M_r values confirm that the $CoAl_2O_4$nano- and microcrystals have soft and weak ferromagnetic nature of the samples [44].

Table 4.2.2. Magnetic measurement results of saturation magnetization (M_s), coercivity (H_c) and remanent magnetization (M_r) of spinel $CoAl_2O_4$ nano and microcrystals

Samples	H_c (O_e)	M_r (emu/g) × 10^{-3}	M_s (emu/g) × 10^{-3}
$CoAl_2O_4$-MCM	299.95	49.23	43.26
$CoAl_2O_4$-SCM	278.21	11.69	19.34

4.2.3.9 Catalytic tests

The catalytic performance of the spinel $CoAl_2O_4$ nano- and microstructures were evaluated in the oxidation of benzyl alcohol in presence of 30 % H_2O_2 as oxidant. In the catalytic oxidation reaction, benzyl alcohol (5 mmol), H_2O_2 (5 mmol) as the oxidant were added with 0.5 g of heterogeneous catalyst and the contents were heated at 80 °C in the presence of acetonitrile (5 mmol) as the solvent for 5 h. Catalytic results showed that the particle size and surface area of the catalyst had a strong influence on both the conversion and product selectivity. The catalytic results were summarized in Table 4.2.3. The resultant catalysts prepared by two different methods display clear difference in the selective oxidation of

benzyl alcohol. It was found that the conversion and product selectivity of benzyl alcohol into benzaldehyde for the sample $CoAl_2O_4$-MCM was higher than that of $CoAl_2O_4$-SCM. It is mainly due to the uniform distribution with smaller particle size of $CoAl_2O_4$-MCM nano-catalyst. The oxidation of benzyl alcohol into benzaldehyde was achieved with 95.73 % conversion and 100 % selectivity of benzaldehyde using the $CoAl_2O_4$-MCM catalyst, which is higher conversion than that of $CoAl_2O_4$-SCM (conversion 64.52 % with 100 % selectivity).

The surface area of nano- and microstructures of $CoAl_2O_4$-MCM and $CoAl_2O_4$-SCM samples are 68.27 m^2/g and 37.53 m^2/g, respectively. Generally, a high specific surface area has a favorable effect on the activity for catalysis. The observed higher efficiency of $CoAl_2O_4$-MCM catalyst in this oxidation reaction can be attributed to the high dispersity and large surface area provides more active sites for catalytic reaction [45]. High specific surface area of $CoAl_2O_4$-MCM (68.27 m^2/g) was useful to catalytic activity via enhancing the adsorption of benzyl alcohol, which is the determining step in the catalytic reaction [46]. However, the sample $CoAl_2O_4$-SCM shows poor performance, due to the bigger particle size with lower surface area (37.53 m^2/g). In MCM approach, the product is formed within few minutes of time with homogeneous and small particle size with higher surface area, which enhance the catalytic activity. In addition, when the surface area increases, the amount of the dispersion of particles per volume in the solution will increase, this result enhances the catalytic activity.

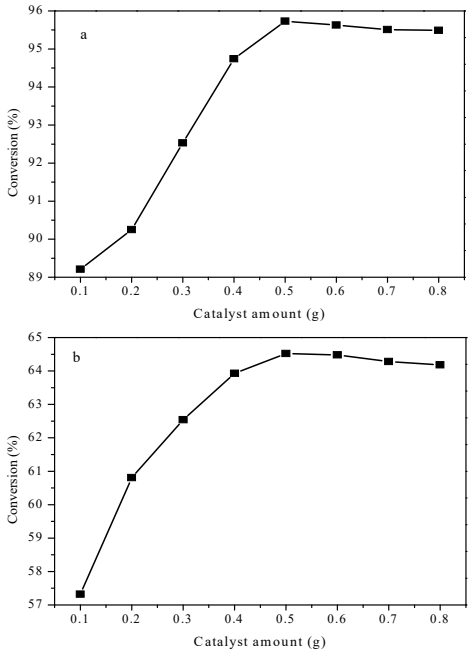

Figure 4.2.9. The amount of spinel catalysts of $CoAl_2O_4$-MCM (Fig. 9a) and $CoAl_2O_4$-SCM (Fig. 4.2.9b) samples on the conversion towards the oxidation of benzyl alcohol into benzaldehyde (Reaction conditions: Catalyst (0.1g to 0.8 g); Benzyl alcohol, 5mmol; Acetonitrile, 5mmol; H_2O_2, 5mmol; Temperature, 80°C, time, 5h).

Usually, the catalytic oxidation of benzyl alcohol produces a mixture of carbonyls and carboxylic acids. However, carboxylic acid is not obtained in the present study. Therefore, the heterogeneous catalyst was found to be highly selective. The catalytic properties of spinel $CoAl_2O_4$ heterogeneous catalyst crucially depend on the distribution of cations among the tetrahedral (A-) and octahedral (B-) sites of the spinel lattice. Moreover, the divalent cations (Co^{2+}) play a vital role in the H_2O_2 decompositions, where the finally produced O_2 would greatly benefit for the oxidation of benzyl alcohol [45].

Table 4.2.3. The conversion and selectivity percentage for the oxidation of benzyl alcohol into benzaldehyde (Reaction conditions: Catalyst ($CoAl_2O_4$-MCM and $CoAl_2O_4$-SCM), 0.5 g; Benzyl alcohol, 5 mmol; Acetonitrile, 5 mmol; H_2O_2, 5 mmol; Temperature, 80 °C, time, 5 h).

Samples	BET surface area (m^2/g)	Conversion (%)	Selectivity(%)
$CoAl_2O_4$-MCM	68.27	95.73	100
$CoAl_2O_4$-SCM	37.53	64.52	100

Fig. 4.2.9a,b shows the influence of the catalyst amount on the conversion towards the oxidation of benzyl alcohol into benzaldehyde. The conversion is gradually increased with increase in the amount of catalyst from 0.1 g to 0.5 g, (Reaction conditions: Catalyst, 0.1 g to 0.8 g; benzyl alcohol, 5 mmol; Acetonitrile, 5 mmol; H_2O_2, 5 mmol; temperature, 80 °C, time, 5 h), and further increase the catalyst amount (0.6 g to 0.8 g), the conversion and yield remain nearly the same, which suggests that large amount of catalyst, is not needed to improve the reaction product [47]. However, it is found that with the increase of catalyst amount the conversion and yield increases upto 0.5 g and this may apparently due to

the availability of more active sites of the catalyst. Therefore, the optimized catalyst amount for the reaction is 0.5 g. The results of the present study indicate that an appropriate conversion and selectivity was obtained even with the small amount of catalyst 0.5 g.

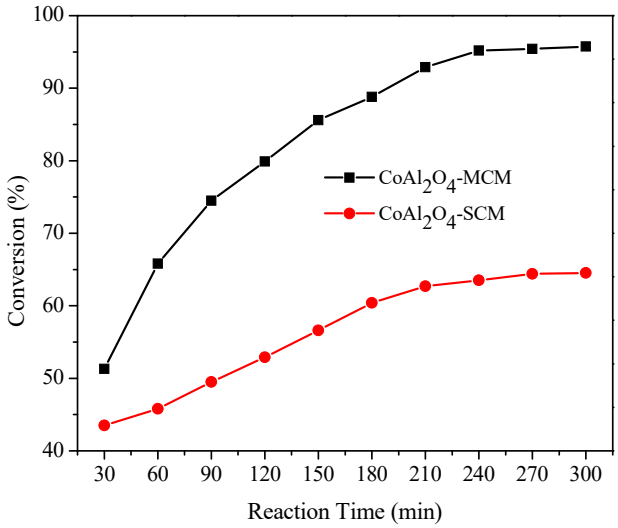

Figure 4.2.10. The catalytic reaction time of $CoAl_2O_4$-MCM and $CoAl_2O_4$-SCM samples on the conversion towards the oxidation of benzyl alcohol into benzaldehyde (Reaction conditions: Catalyst (0.1g to 0.8 g); Benzyl alcohol, 5 mmol; Acetonitrile, 5 mmol; H_2O_2, 5 mmol; Temperature, 80 °C, time, 5 h).

Catalytic reaction time is very important to measure the activity. Fig. 4.2.10 shows the effect of reaction time on the conversion of benzyl alcohol into benzaldehyde using heterogeneous ($CoAl_2O_4$-MCM and $CoAl_2O_4$-SCM) catalyst. It was found that the conversion increased linearly with increasing the reaction time up to 180 min and then increased slowly from 180 to 240 min. The product conversion was found to be nearly same for the 240 and 300 min experiments, indicating the constant conversion after 240 min. No significant change in the oxidation of benzyl alcohol was observed when running the reaction for 300 min [47]. However, the catalytic activity of $CoAl_2O_4$-MCM is higher than other samples, due to that with very smaller particle size distribution would be a potentially efficient catalyst [48].

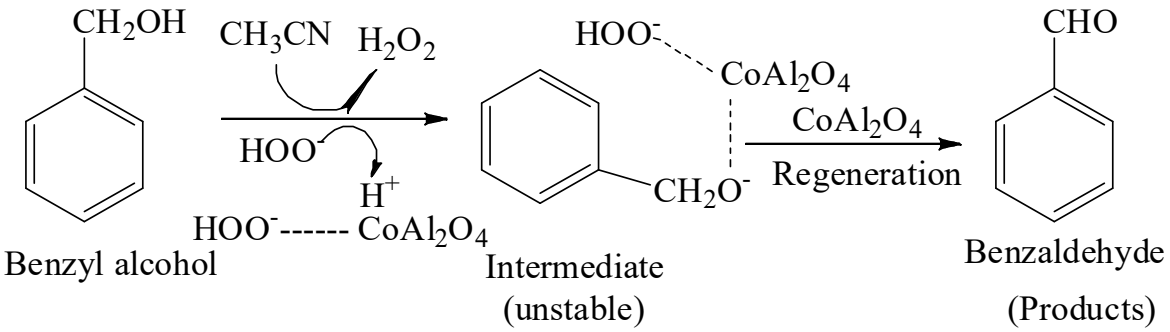

Figure 4.2.11. Schematic diagram of catalytic oxidation of benzyl alcohol into benzaldehyde by spinel $CoAl_2O_4$ catalyst.

The proposed catalytic oxidation reaction mechanism for $CoAl_2O_4$ catalyzed reaction of acetonitrile medium as shown in Fig. 4.2.11. Originally, the solvent CH_3CN can activate oxidant H_2O_2 by forming a perhydroxyl anion, OOH^- to generate an intermediate peroxycarboximidic acid. The catalyst reacts with the H_2O_2 molecule to form Co-OOH^- as an initiation step. This perhydroxyl species, which are formed on the surface of the catalyst, will then oxidize the alcohols substrates. It is well known that the formed intermediate peroxy carboximidic acid is a good oxygen transfer agent. The benzyl alcohol and the H_2O_2 dissolve in CH_3CN, which activate H_2O_2 to OOH^- anion and forming Co-OOH^- species [49]. This account revealed that the OH group of benzyl alcohols interacts with the Co^{2+} ion. The contact of the OH group with the Co^{2+} ions in $CoAl_2O_4$ is also clear by the adsorption of phenyl ring on catalyst. However, the $CoAl_2O_4$ catalyst surface gets regenerated by the action of H_2O_2, which leads to desorption of the product carbonyls, thus favor further oxidation. In addition, H_2O_2 has been proved to be efficient, environmentally friendly oxidant, since the product is only carbonyls [47, 48].

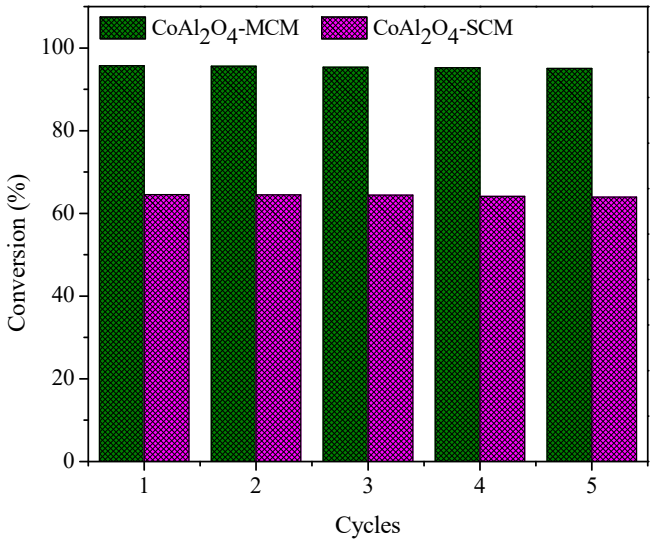

Figure 4.2.12. The reusability of the spinel catalysts ($CoAl_2O_4$-MCM and $CoAl_2O_4$-SCM) for the catalytic oxidation of benzyl alcohol into benzaldehyde.

4.2.3.10 Reusability studies

The catalytic oxidation of benzyl alcohol into benzaldehyde was employed as a model reaction to investigate the reusability of spinel $CoAl_2O_4$ nano and microcrystal catalysts. The recycling of the catalyst is very important for industrial and technological applications. The reusability of the catalyst for the liquid phase oxidation of benzyl alcohol into benzaldehyde was evaluated and the results are shown in Fig. 4.2.12. For the reusability study purpose, the sample spinel $CoAl_2O_4$ nano and microcrystal catalysts was filtered off from each run and washed several times with ethanol and dried at 110 °C in an air oven for 1 h and was checked for five consecutive runs under the identical conditions. During the five runs investigated, the conversion of benzyl alcohol into benzaldehyde was in the range from 95.73 to 95.25 % for the sample $CoAl_2O_4$-MCM (Fig. 4.2.12), indicating that these catalyst displays good reproducibility and stability. Interestingly the formation of benzoic acid was not detected. However, it was observed that the conversion of benzyl alcohol into benzaldehyde was in the range from 64.52 to 63.93 % for the sample $CoAl_2O_4$-SCM (Fig. 4.2.12). Since, the spinel $CoAl_2O_4$nano-catalyst is able to oxidize benzyl

alcohol into benzaldehyde with high activity, highly recyclable, remarkably stable and environmental friendly; they are promising candidates for the industrial applications.

4.2.4. Conclusions

In this chapter, we proposed a fast and non-polluting method to prepare spinel $CoAl_2O_4$ nanostructured catalysts by microwave combustion method (MCM), in which glycine was successfully used as a fuel. For the comparative study, it was also prepared by solution combustion method (SCM). MCM approach is extremely facile and offers an inexpensive method than SCM route. Powder XRD, FT-IR, EDX spectra, SAED, HR-SEM and HR-TEM results showed that the as-prepared samples were pure phase spinel $CoAl_2O_4$nano- and microstructures without any other secondary phase impurity. The calculated optical band gap value of the samples $CoAl_2O_4$-MCM is 3.72 eV, which is higher than the sample $CoAl_2O_4$-SCM (3.39 eV). The relatively lower M_s (19.34×10^{-3} emu/g) of $CoAl_2O_4$-SCM shows that it is weak ferromagnetic in nature and high M_s (43.26×10^{-3} emu/g) of $CoAl_2O_4$-MCM confirms its ferromagnetic behavior. It was found that the sample $CoAl_2O_4$-MCM show higher conversion (95.73 %) of benzyl alcohol into benzaldehyde than $CoAl_2O_4$-SCM (64.52 %), due to the smaller particle size and higher surface area. Moreover, the MCM approach provides a simple and convenient method than that of SCM technique for preparing the transition spinel metal oxides. The synthetic route (MCM approach) can be further used for the synthesis of other nano metal oxides.

References

[1] B. Bhushan (Ed.), Hand book of Nanotechnology, 3rd edition, Springer, Germany (2010).

[2] Jan. G. Korvink and Andreas Greiner, Semiconductors for micro and nanotechnology: An introduction for engineers, Wiely (2002).

[3] Rainer Wasser (Ed.), Nanotechnology: Volume 3: Information technology 1, Wiely-VCH (2008).

[4] K. Bogunia-Kubik and M. Sugisaka, From molecular biology to nanotechnology and nanomedicine, Biosystems 65, 123 (2002).

[5] Alexandra Navrotsky, Materials and nanotechnology, J. Franklin Institute 340, 263 (2003).

[6] L. Mazzola, "Commercializing nanotechnology", Nature Biotechnol.,21, 1137 (2003).

[7] A. Stein, "Energy storage: Batteries take charge", Nature Nanotechnol.,6, 262 (2011).

[8] J. Garcia-Martinez (Ed.), Nanotechnology for the energy challenge, Wiley- VCH, (2010). DOI: 10.1002/9783527629299.ch1.

[9] M. Henini, Focus on Nanotechnology,11, 30 (1998).

[10] M. Wiesner and J-Y.Bottero, McGraw-Hill (2007).

[11] M. Geller, F. Hopfer and D. Bimberg, Microelectronics journal,39, 302 (2008).

[12] S.K Sahoo, S. Parveen and J.J Panda, Nanomedicine,3, 20 (2007).

[13] M.R. Mohamadi, L. Mahmoudian, N. Kaji, M. Tokeshi, H. Chuman and Y. Baba, Nanotoday,1, 38 (2006).

[14] L.M. Smith, Nature, 465, 167 (2010).

[15] D. Minoli, Wiely& Sons, NewJersy (2006).